
1 The relative importance of antecedent soil moisture and precipitation
2 in flood generation in the middle and lower Yangtze River basin

3

4 ~~Qihua Ran~~Sheng Ye¹, Jin ~~Wang~~¹Wang², ~~Qihua Ran~~^{2*}, Xiuxiu ~~Chen~~¹Chen², Lin
5 ~~Liu~~¹Liu², Jiyu ~~Li~~¹—Li², Sheng Ye^{2*}

6

7 ¹ State Key Laboratory of Hydrology-Water Resources and Hydraulic Engineering,
8 Hohai University, Nanjing 210098, China

带格式的: 行距: 2 倍行距

9 ² Institute of Water Science and Engineering~~Water Resources~~, College of Civil
10 Engineering and Architecture, Zhejiang University, Hangzhou 310058, China

11

12 * Corresponding author: Sheng Ye

13

14 Email address of the corresponding author: yesheng@zju.edu.cn

15

16 September 8, 2022

17

18

19

20 **Abstract**

21 Floods have caused severe environmental and social economic losses worldwide in
22 human history, and are projected to exacerbate due to climate change. Many floods are
23 caused by heavy rainfall with highly saturated soil, however, the relative importance of
24 rainfall and antecedent soil moisture and how it changes from place to place has not
25 been fully understood. Here we examined annual floods from more than 200
26 hydrological stations in the middle and lower Yangtze River basin. Our results indicate
27 that the dominant factor of flood generation shifts from rainfall to antecedent soil
28 moisture with the increase of watershed area. The ratio of the relative importance of
29 antecedent soil moisture and daily rainfall (SPR) is positively correlated with
30 topographic wetness index and has a negative correlation with the magnitude of annual
31 floods. This linkage between watershed characteristics that are easy to measure and the
32 dominant flood generation mechanism provides a framework to quantitatively estimate
33 potential flood risk in ungauged watersheds in the middle and lower Yangtze River
34 basin.

35 **Key words:** flood generation, scaling effect, topographic wetness index

36

37

38 **1. Introduction**

39 Flooding is one of the most destructive and costly natural hazards in the world, resulting
40 in considerable fatalities and property losses (Suresh et al., 2013). River floods have
41 affected nearly 2.5 billion people between 1994 and 2013 worldwide (CRED, 2015),
42 and caused 104 billion dollars losses every year (Desai et al 2015). The damages may
43 be further exacerbated by increasing frequency and intensity of extreme rainfall events
44 according to climate change projections (IPCC 2012; Ohmura and Wild 2002). Flood
45 control infrastructures and more accurate predictions are needed to reduce flood
46 damages, which requires better understanding of the underlying mechanism of flood
47 generation as well as the drivers of change (Villarini & Wasko 2021).

48 Numerous studies have been conducted to investigate the cause of floods across
49 the world (Bloschl et al 2013; Munoz et al 2018; Zhang et al 2018). Many studies
50 focused on examining the environmental and social characteristics that lead to specific
51 catastrophic flood events (Bloschl et al 2013; Liu et al 2020; Zhang et al., 2018). Others
52 concentrated on single locations, usually catchment outlets, to explore the influential
53 factors of floods and the future trends (Brunner et al., 2016; Munoz et al 2018). Yet
54 given the amount of data and time required, it is not practical to apply these detailed
55 studies to hundreds of catchments to generate an overview of the flood generation
56 mechanism at large scale.

57 Recently, researchers started to investigate the dominant flood generation
58 mechanisms at regional scales (Berghuijs et al 2019b; Do et al 2020; Garg & Mishra
59 2019; Smith et al 2018; Tramblay et al 2021; Ye et al 2017). Most of these studies are
60 conducted in North America and Europe with well-documented long-term records
61 (Berghuijs et al 2016; Bloschl et al 2019; Do et al 2020; Musselman et al 2018; Rottler

62 et al 2020). Some research was conducted in China recently (Yang et al 2019; Yang et
63 al 2020), though such kind of work is still limited, further investigations are needed
64 given the considerable spatial heterogeneity and complexity in flood generation.

65 As the largest river in China, Yangtze River basin has long suffered from floods. In
66 summer 2020, 378 tributaries of the Yangtze River had floods exceeding the alarm level,
67 causing billions of dollars damage (Xia et al., 2021). With the increasing public
68 awareness, more accurate prediction is needed, which relies on better understanding.
69 However, due to the limitation of observations, there are only a few regional studies of
70 the flood generation mechanism in China, with few in the Yangtze River basin (Zhang
71 et al 2018; Yang et al 2019; Yang et al 2020). The large number of dams and reservoirs
72 built along the river further complicated the situation (Feng et al., 2017; Qian et al 2011;
73 Yang et al 2019).

74 Because of the relatively warm temperature, snowmelt has little impact on flood
75 generation in the Yangtze River basin (Yang et al 2020). Floods in the Yangtze River
76 basin usually occur during summer with relatively wet soil and high rainfall (Wang et
77 al 2021). Heavy rainfall with high antecedent soil moisture has also been identified as
78 dominant driver of floods across world (Beighuijs et al 2019b; Garg et al 2019;
79 Trambly et al 2021; Wasko et al 2020). Recently, studies started to examines the
80 relative importance of rainfall and antecedent soil moisture in flood generation
81 (Brunner et al., 2021; Wasko et al., 2021; Bennett et al., 2018; Bertola et al., 2021).
82 Quantitative evaluation of the relative contribution of rainfall and antecedent soil
83 moisture and its change across watersheds is still limited and currently unavailable in
84 China (Liu et al., 2021; Wu et al., 2015).

85 Based on the watersheds in the middle and lower Yangtze River basin, this study

86 attempts to explore the following questions: 1) is there a way to quantitatively describe
87 the relative importance of antecedent soil moisture and rainfall on flood generation; and
88 2) how would this combination of flood-generation rainfall and soil moisture vary
89 across watersheds, and what are the influential factors. Based on the observations and
90 model estimation (Section 2), the spatial distribution patterns of antecedent soil
91 moisture and rainfall were obtained and analyzed to investigate their individual
92 contribution to flood generation and the influential factors (Section 3). This allows for
93 further examination of the relative importance of antecedent soil moisture and rainfall
94 on flood generation and its linkage to watershed characteristics as well as its
95 implications to flood prediction (Section 4), all the results are summarized in Section 5.

96 **2 Methods**

97 **2.1 Study area**

98 The Yangtze River is the largest river in China, with a total length of 6,300 kilometers
99 and annual discharge of 920km³ at the outlet (Yang et al., 2018). It drains through an
100 area of 1.8*10⁶ km², lying between 90°33' and 122°25'E and 24°30' and 35°45'N, and
101 is home to over 400 million people, most of which live in the middle and lower Yangtze
102 River basin (YZRB) (Cai et al., 2020). The elevation of the YZRB declines from west
103 to east: from over 3000m in Qinghai-Tibet Plateau, to around 1000m in the central
104 mountain region, and the 100m in Eastern China Plain (Wang et al., 2013). The
105 vegetation types in the YZRB are forests, shrubs, grassland and agricultural land,
106 accounting for 11.85%, 12.65%, 32.26% and 42.88% respectively. Grassland and
107 shrubs are the dominant vegetation in the middle and upper YZRB, while the
108 downstream YZRB is dominated by forests and agricultural land (Miao et al., 2010).
109 There are more than 51,000 reservoirs of different sizes in the whole basin, including

110 280 large ones (Peng et al., 2020).

111 Most of the YZRB is semi-humid and humid, with a typical subtropical monsoon
112 climate. The mean annual temperature is approximately 13.0 °C, varying from -4 °C
113 to 18°C downstream. The mean annual precipitation of the whole basin is about 1200
114 mm, increasing from 300mm in the western headwaters to 2400 mm downstream. (Li
115 et al., 2021). Most of the precipitation comes between June and September, the premise
116 of persistent heavy rain in the Yangtze River basin is the frequent activity of weak cold
117 air in the north (Tao et al., 1980) and the intersection of mid-latitude air mass and
118 monsoon air mass (Kato et al., 1985). Studies have found that both annual precipitation
119 and the frequency of extreme precipitation events have increased in the middle and
120 lower reaches of the Yangtze River (Qian et al., 2020; Fu et al., 2013). As a result, floods
121 have occurred frequently in the middle and lower reaches of the Yangtze River, where
122 most of the population in the YZRB live (Liu et al., 2018).

123 **2.2 Data**

124 In this work, we focus on the middle and lower reaches of the Yangtze River for the
125 high population density and increasing flood risk. The 30-meter digital elevation model
126 (DEM) was downloaded from Geospatial Data Cloud (<http://www.gscloud.cn/>), from
127 which the drainage area corresponding to the hydrological station was extracted by
128 ArcGIS. Daily precipitation data and temperature data between 1970 and 2016 from
129 247 meteorological stations within and near the YZRB were downloaded from China
130 Meteorological Data Network (<https://data.cma.cn/>) (Figure 1). The temperature data
131 was used to estimate potential evaporation. The observed precipitation and estimated
132 potential evaporation were interpolated into the whole YZRB using the Thiessen
133 polygon method (Meena et al., 2013). The interpolated precipitation and potential

134 evaporation were then averaged for the drainage area corresponding to each
135 hydrological station.

136 The daily streamflow data was collected from 267 hydrological stations from
137 Annual Hydrological Report of the People's Republic of China. Among which, 224
138 stations with at least 20 years records from both the period from 1970 to 1990 and the
139 period from 2007 to 2016 were selected, the data from 1990 to 2007 were not found in
140 online repository (see Figure S1 for data availability). Information of 361 reservoirs in
141 the middle and lower YZRB, including capacity and controlling area was downloaded
142 and extracted from the Global Reservoir and Dam database (GRanD) (Lehner et al
143 2011). Previous study showed that this database provides reliable information of middle
144 and large reservoirs in China (Yang et al 2021). Watersheds with more than 80% of the
145 drainage area under control reservoirs according to GRanD database and/or located
146 right downstream of reservoirs and water gates were considered as watersheds under
147 strong regulation (regulated watersheds).

148 **2.3 Calculation of hydrological and topographic characteristics**

149 *Potential evaporation estimation*

150 The temperature data was used to estimate potential evaporation following the
151 Hargreaves method (Allen et al., 1998; Vicente et al., 2014; Berti et al., 2014).

$$152 \quad ET_0 = 0.0023 \times (T_{max} - T_{min})^{0.5} \times (T_{mean} + 17.8) \times Ra \quad (1)$$

153 where ET_0 is potential evaporation (mm/d), T_{max} is the highest temperature ($^{\circ}\text{C}$), T_{min}
154 is the lowest temperature ($^{\circ}\text{C}$), T_{mean} is the mean temperature ($^{\circ}\text{C}$), and Ra is the outer
155 space radiation [$\text{MJ}/(\text{m}^2 \cdot \text{d})$], which can be calculated as follows:

156
$$Ra = 37.6 \times d_r \times (\omega_s \sin \varphi \sin \delta + \cos \varphi \cos \delta \sin \omega_s), \quad (2)$$

157 where d_r is the reciprocal of the relative distance between the sun and the earth, ω_s is
158 the angle of sunshine hours, δ is the inclination of the sun (rad), φ is geographic
159 latitude (rad). d_r , δ and ω_s can be calculated by the following formula:

160
$$d_r = 1 + 0.033 \times \cos\left(\frac{2\pi J}{365}\right), \quad (3)$$

161
$$\delta = 0.409 \times \sin\left(\frac{2\pi J}{365} - 1.39\right), \quad (4)$$

162
$$\omega_s = \arccos(-\tan \varphi \tan \delta), \quad (5)$$

163 where J is the daily ordinal number (January 1st is 1).

164 *Soil water storage estimation*

165 The soil water storage was estimated based on the daily water balance (Berhuijs et al.,
166 2016, 2019):

167
$$\frac{dS}{dt} = P - ET - \max(Q, 0), \quad (6)$$

168 Where S is the soil water storage (mm), which is initially set to 0. Due to the long term
169 of simulation, the change of initial value would not significantly affect the results. P is
170 precipitation (mm/d), Q is discharge normalized by area (mm/d), ET is evaporation
171 (mm/d), which can be calculated from potential evapotranspiration (ET_0), where the
172 soil water storage (S) is used as the upper limit of daily ET:

173
$$ET = \min(0.75 \times ET_0, S), \quad (7)$$

174 The estimation of soil water storage and ET are highly simplified and is not used for

175 prediction but to capture the first order of the temporal variation and the relative
176 wetness of soil in the study time period, which helps develop a framework that
177 differentiates the relative contribution of precipitation and soil moisture in flood
178 generation.

179 *Topographic wetness index estimation*

180 Topographic wetness index was calculated to represent the combined impacts of
181 drainage area and topographic gradient (Alfonso et al., 2011; Grabs et al., 2009):

$$182 \quad \quad \quad TWI = \ln(A_d/\tan\alpha), \quad (8)$$

183 where A_d is drainage area and α is topographic gradient estimated from DEM. TWI
184 represents the propensity of subsurface flow accumulation and frequency of saturated
185 conditions, thus can be used to predict relative surface wetness and hydrological
186 responses (Meles et al 2020). It is widely used to quantify topographic impact on
187 hydrological processes (i.e., spatial scale effects, hydrological flow path, etc.), as well
188 as in land surface models for hydrological, biogeochemical and ecological processes
189 (Sorensen et al 2006).

190 **2.4 Quantification of the relative importance of soil moisture and precipitation** 191 **during floods**

192 The maximum daily discharge of each year was selected as annual flood, which was
193 then averaged across years as the mean annual maximum flood (AMF). The observed
194 rainfall on that day and the estimated soil water storage at the day before AMF in each
195 year were also averaged across years as daily rainfall (P) and antecedent soil moisture
196 (S_0). Since almost all the AMFs in our study region come during rainy season when
197 rainfall comes in most of the days, it could be difficult to isolate the events of AMFs

198 among consecutive flow events. To avoid the bias that may be caused in event
199 separation, the soil moisture at the day before AMF was used as antecedent soil
200 moisture, instead of the day before the event of AMF. To examine the impacts from
201 long-lasting rainfall event, especially for the large watersheds with longer concentration
202 time, we also calculated the mean accumulated rainfall from two days (rainfall on the
203 flood day and the day before, P_2) to seven days before (weekly rainfall, P_7).

204 The percentile of antecedent soil moisture (S_{θ}) was calculated to represent the
205 relative saturation of soil moisture in the time series; while the percentile of daily
206 rainfall (P) was estimated to show the relative intensity (P'), representing the relative
207 magnitude of rainfall events across time. The percentile of accumulated rainfall was
208 also calculated for the two-day to seven-day rainfall.

209 To quantify the relative importance of antecedent soil moisture and rainfall in flood
210 generation, the ratio between these two factors at the AMFs was derived: $SPR = S'/P'$.
211 When SPR is large, the antecedent soil moisture is much closer to the maximum, while
212 the daily rainfall is less extreme, floods are more affected by the antecedent soil
213 moisture. On the other hand, a smaller SPR indicates relatively larger magnitude of
214 rainfall comparing with antecedent soil moisture, that is, rainfall is more extreme and
215 influential in flood generation.

216 **3 Results**

217 **3.1 Spatial patterns of antecedent soil moisture and precipitation during floods**

218 Figure 2 shows the spatial distribution of the percentile of antecedent soil moisture and
219 daily rainfall during the annual maximum floods (AMFs) in the middle and lower
220 reaches of the Yangtze River. As we can see from Figure 2a, in the middle and lower

221 reaches of YZRB, when AMFs occurred, the percentile of antecedent soil saturation
222 was generally high, most of them are larger than 0.6: the farther away from the main
223 stream, the more saturated the soil was. On the other hand, along and near the main
224 stream and the delta, the antecedent soil saturation rate could be much smaller, even
225 less than 0.4.

226 Figure 2b shows the daily rainfall during the AMFs. As we can see, the percentile
227 of daily rainfall is relatively high (>0.8) at more than half of the study sites, while it is
228 small (<0.5) for the sites along the main stream and in the delta (Figure 2b). Comparison
229 between Figure 2a and b suggests that, except the sites on the main stream and in the
230 delta, sites with relatively high antecedent soil saturation rate (i.e., >0.8 , the blue dots)
231 during AMFs are also the ones with relatively small daily rainfall contribution (i.e.,
232 <0.8 , the light blue and cyan dots). That is, for these sites, the AMFs are usually
233 occurring at a much wetter condition while extreme rainfall at flood day is not necessary,
234 suggesting the relative importance of soil wetness. For the sites with both the percentile
235 of soil moisture and rainfall between 0.6 and 1, both the antecedent soil moisture and
236 rainfall play important roles in flood generation. As for the sites on the main stream and
237 in the delta, both antecedent soil moisture and rainfall are low during AMFs, this is
238 likely due to the regulations from large reservoirs and water gates.

239 **3.2 The scaling effect in the contribution of antecedent soil moisture and rainfall**

240 To further investigate the relative importance of antecedent soil moisture and rainfall
241 in flood generation and the potential influential factors, we examined their correlation
242 with catchment area (Figure 3). Given the complicated environmental and social
243 impacts, the regulated watersheds and sites on the main stream are presented separately
244 (the green dots and cyan dots in Figure 3 respectively). Our study will focus on the sites

245 that are not dominated by regulation (the blue dots in Figure 3), for simplicity, we will
246 refer them as natural watersheds.

247 As we can see from Figure 3, during the occurrence of AMFs, the percentile of
248 antecedent soil wetness increases with watershed area (p -value<0.001), while the
249 percentile of daily rainfall decreases with watershed area (p -value<0.001). That is, with
250 the increase of watershed size, antecedent soil moisture becomes more and more
251 saturated while the precipitation is less and less extreme during AMFs; suggesting the
252 rising contribution of antecedent soil moisture and declining importance of daily
253 precipitation in flood generation. As for the regulated watersheds (green dots in Figure
254 3), there is no clear correlation between drainage area and the percentile of antecedent
255 soil moisture or rainfall, which is understandable. Meanwhile, both the percentile of
256 antecedent soil moisture and rainfall decreases with watershed area for main stream
257 sites.

258 3.3 The scaling impacts on accumulated rainfall

259 The saturation of soil before floods could be due to previous rainfall events, and could
260 also be caused by accumulated rainfall in long-lasting rainfall events that eventually
261 generate floods (Xie et al., 2018). Figure 4 presents the correlation between the
262 percentile of accumulated rainfall and drainage area. When single day rainfall is
263 considered, it is negatively correlated with drainage area (Figure 3a); when
264 accumulated rainfall is considered, the correlation gradually shifts from negative to
265 positive correlation (Figure 4). For example, when two-day rainfall was examined, the
266 correlation between accumulated rainfall and drainage area shifts from negative to
267 positive at 10,000 km²; the negative correlation in Figure 3a is only valid for watersheds
268 larger than 10,000 km² (Figure 4a). This transition area increases from 10,000 km² for

269 two-day rainfall to 100,000 km² for four-day rainfall (Figure 4c). The number of
270 watersheds with negative correlation also decreases. Eventually, the weekly rainfall has
271 similar positive correlation with drainage area like antecedent soil moisture (Figure 4f).
272 The increase of transition area may be explained by the increasing response time and
273 confluence time in large watersheds: it takes days to generate flow events by heavy
274 rainfall and for them to reach outlets where it can be observed in large watersheds. This
275 is also consistent with the conclusion in the Yellow River Basin (Ran et al., 2020) and
276 our previous findings of the dominant flood generation mechanism in the middle and
277 lower YZRB: weekly rainfall is the dominant flood driver for sites on the main streams
278 and the major tributaries (Wang et al 2021). The regulated watersheds don't show
279 significant correlation which is understandable for the strong human intervention. For
280 the negative correlation between accumulated rainfall and drainage area at main stream
281 sites, it is difficult to decide whether it is due to scaling effect or human intervention.

282 **3.4 The interlink of watershed characteristics, flood, antecedent soil moisture and** 283 **rainfall**

284 Figure 5 presents the percentile of antecedent soil moisture and rainfall during the
285 AMFs at the study watersheds, the circles are scaled by watershed size and colored with
286 topographic gradient. Except the watersheds with strong human intervention (regulated
287 ones and the ones on main stream), there is a negative correlation between the
288 contribution of rainfall and antecedent soil moisture. The lower right of the scatter are
289 mostly big blue dots, which are large watersheds with gentle topographic gradient. That
290 is, AMFs usually occur when soil moisture is close to saturation while extreme rainfall
291 is not necessary for AMFs in these watersheds. On top of the scatter are relatively small
292 yellow and green dots, those are medium to small watersheds with steep topographic

293 gradient. That is, AMFs are usually generated with extreme rainfall, while the saturation
294 of soil moisture is not necessary. This negative correlation indicates the shift of
295 dominance in AMFs generation from extreme rainfall to antecedent soil wetness from
296 small steep watersheds to large flat ones.

297 Figure 6 shows the relative importance of antecedent soil moisture and rainfall. For
298 the natural watersheds (the circles), SPR increases with drainage area and declines with
299 topographic gradient. That is, the larger the drainage area is, the more essential the
300 contribution of antecedent soil moisture to floods is, and the less influential rainfall is
301 in flood generation. For watersheds with similar drainage area (i.e., the green or light
302 blue dots in Figure 6b), topographic gradient also cast impacts on SPR: SPR decreases
303 with slope. That is, the relative importance of rainfall increases at steeper watersheds.
304 This may be attributed to the shortened hydrological response time due to the steep
305 topography which facilitates rainfall induced floods generation. As a combination of
306 both drainage area and topographic gradient, TWI is positively correlated with SPR at
307 natural watersheds, with less scatter than the correlation between SPR and drainage
308 area or topographic gradient alone. That is, watersheds with larger area and gentler
309 topographic gradient that are easier to get wet tend to have larger SPR: soil wetness is
310 more important in flood generation. There is no significant correlation between SPR
311 and TWI for the regulated watersheds along tributaries (black triangles). However, the
312 sites on main stream show opposite pattern: the SPR at these sites decreases with TWI
313 and drainage area. It is difficult to determine whether this is because of reservoir
314 regulation or not. More data about watersheds larger than 10,000km² but with limited
315 human intervention are needed to examine this hypothesis.

316 Besides TWI, SPR is also correlated with the magnitude of AMF (Figure 7). As

317 Figure 7 shows, the area normalized flood peak declines with flood-generation SPR.
318 Watersheds with large flood peak are mostly the ones with steep topographic gradient
319 and small SPR (i.e., $SPR < 1$) and vice versa. Catchments with more extreme floods are
320 the ones with relatively less influence of soil moisture on flood generation. Similar
321 correlation was also found at event scale in our experimental mountainous watershed,
322 which locates at a headwater of Yangtze River (Liu et al 2021).

323 **4 Discussion**

324 **4.1 The relative importance of antecedent soil moisture and rainfall in flood** 325 **generation**

326 While soil moisture and rainfall are the two main drivers of floods in the middle and
327 lower Yangtze River basin, the dominance of each factor varies across the relatively
328 natural watersheds. Floods in large watersheds are usually generated when soil is almost
329 saturated despite of the relatively small rainfall amount, while extreme rainfall is
330 usually observed during floods in small to medium watersheds (blue dots in Figure 3).
331 The rising contribution of antecedent soil moisture in large watersheds was consistent
332 with the findings in Australian watersheds (Wasko & Nathan, 2019); and the declining
333 influence of rainfall at larger watersheds was also found in Indian watersheds (Garg et
334 al 2019). This contrast correlation with watershed size indicates a shift of dominance
335 in AMFs generation, which may be attributed to the longer confluence time in the large
336 watersheds and less heterogeneity in small watersheds.

337 This shift of dominance can be observed more straightforwardly from the negative
338 correlation between the percentile of rainfall and antecedent soil moisture in Figure 5.
339 The natural watersheds in Figure 5 could be grouped into three classes based on their

340 drainage area and topographic gradient. When a watershed is large and flat, flood
341 occurrence is mainly determined by soil wetness (i.e., the big blue dots at the lower
342 right of the scatter); on the other hand, when a watershed is small and steep, heavy
343 rainfall takes over the dominance (i.e., the small yellow and green dots at the upper left
344 of the scatter). Between these two groups are relatively small watersheds with gentle
345 topographic gradient, where the occurrence of AMF requires both highly saturated soil
346 and relatively heavy rainfall. That is, the dominant influential factor(s) in AMFs
347 generation across watersheds is correlated with the topographic characteristics (i.e.,
348 watershed size and topographic gradient). This helps quantify the relative importance
349 of soil moisture and rainfall in flood generation in the existing work.

350 This shift of dominance is not observed in the main stream sites (i.e., cyan dots in
351 Figure 3), where the percentile of both antecedent soil moisture and precipitation
352 declines with drainage area. This may be attributed to the more complicated flood
353 generation mechanism at large scale as well as the strong human intervention on main
354 stream (e.g., reservoirs, water gates regulation, etc.) (Gao et al., 2018; Long et al., 2020;
355 Zhang et al., 2017). The major responsibilities of reservoirs on the main stream are to
356 reduce peak flow and postpone the time to flood peak (Volpi et al., 2018). As a result,
357 the original flood peak would be delayed by regulation and the actual flood peak would
358 occur when rainfall declines/stops and soil water drains. Another possibility is that
359 when watershed size is larger than 100,000km², the impact of antecedent soil moisture
360 declines as well. To examine this hypothesis, more data from watersheds larger than
361 100,000km² and with limited human intervention is needed. However, this is above the
362 scope of this work and requires future studies.

363 4.2 Linkage between topographic characteristics, SPR and floods

364 The correlation between TWI and SPR (Figure 6c) demonstrates that the relative
365 importance of soil moisture and rainfall could be inferred from topographic
366 characteristics quantitatively. We could derive the relative dominance of soil moisture
367 and rainfall in flood generation in specific watershed from its TWI for the natural
368 watersheds without significant human intervention. Rainfall and soil moisture level
369 have been identified as dominant drivers of floods, individually or together, in
370 watersheds worldwide (Berghuijs et al 2016, 2019b; Garg & Mishra 2019; Trambly et
371 al 2021; Ye et al 2017). Our findings provide a framework to quantify the relative
372 importance of rainfall and soil moisture and to further identify the influential factors of
373 their importance based on topographic characteristics that are easy to measure.

374 Meanwhile, the SPR also present a negative correlation with the magnitude of
375 AMFs (Figure 7). That is, we could infer the mean annual AMF based on SPR for each
376 watershed. Since the characteristic SPR could be estimated from TWI, we could derive
377 quantitative estimation of the mean AMFs from topographic characteristics that are
378 easy to measure, even in watersheds with little hydrologic records. There is also similar
379 negative correlation between TWI and AMFs (Figure S2). This would be helpful for
380 flood control management in ungauged watersheds, especially in the mountainous
381 watersheds with risks of flash floods. Similar correlation was also found in the
382 observations from our experimental watershed, a headwater of Yangtze River (Liu et al
383 2021). The ratio of observed antecedent soil moisture and event precipitation also
384 presents similar decline trend with discharge at event scale. However, the correlation
385 between SPR and discharge at event scale is preliminary, more data with higher
386 resolution and detailed analysis are needed for validation at event scale. For this study,
387 our goal is to present the framework to derive flood generation SPR that could be
388 estimated from topographic characteristics and to provide information of mean AMFs.

389 In conclusion, based on the topographic characteristics, we could derive the relative
390 importance of soil moisture and rainfall in flood generation (SPR); and from this
391 relative importance ratio, we could further infer the average flood magnitude at these
392 watersheds. As a result, we could link the topographic characteristics and annual floods
393 through the characteristic SPR during the AMFs.

394 **4.3 Implications**

395 Our findings could be helpful for potential flood risk evaluation in ungauged basins,
396 e.g., headwaters in the mountainous region. With the construction of large reservoirs,
397 the capability of flood risk control has improved substantially along the main stream
398 (Zou et al., 2011; Zhang et al., 2015). However, it is still difficult for quantitative
399 evaluation of flood risk in upstream mountainous watersheds, which are vulnerable to
400 floods but difficult for hydrological modeling and prediction due to little hydrologic
401 records.

402 Our findings suggest that we could derive the flood-generation SPR of each
403 watershed from drainage area and topographic gradient that are easy to measure. The
404 correlation between SPR and flood peak provides information of the mean annual
405 floods in ungauged watersheds. Therefore, in regions without observation data, to build
406 flood control infrastructure such as dams and gates, the mean annual flood peak
407 obtained by SPR based on the topographic characteristics can be used to provide
408 quantitative information for flood control and disaster management. Flood control
409 infrastructures could be designed based on the estimated mean annual flood peak as
410 well as the demographic information. With further validation of this framework at event
411 scale, by using the observed soil moisture from remote sensing data and precipitation
412 forecast to generate real-time prediction of SPR values, we could further provide early

413 warning of floods in these ungauged watersheds. This would be helpful given the
414 increasing possibility of extreme rainfall events due to climate change, however, more
415 data and examination are needed in future studies.

416 **4.4 Limitations**

417 Previous works usually identify the dominant flood generation mechanism based on the
418 comparison of the timing of events (Berghuijs et al 2016; 2019b; Bloschl et al 2017; Ye
419 et al 2017). Similar work has been implemented in our study watersheds, suggesting
420 the importance of soil moisture and rainfall (Wang et al 2021). Based on that, we further
421 looked into the records to quantitatively evaluate the relative importance of soil
422 moisture and rainfall in flood generation. However, there are limitations in our methods.

423 The precipitation data we used were averaged for the study watersheds from 247
424 meteorological stations. Given the large area and considerable spatial heterogeneity, the
425 precipitation data we used may not always be representative of the actual precipitation
426 events. The daily data could also average the rainfall intensity at hourly scale, which
427 could be influential in small mountainous watersheds. ET was scaled as $0.75*ET_0$ to
428 make sure it is smaller than the potential evaporation. This is a simplified estimation of
429 ET; more sophisticated method is needed in further analysis on specific catchments at
430 event scale.

431 The estimation of soil moisture is also highly simplified, which cannot be
432 considered as precise estimation at event scale. To reduce the influence from this
433 simplification, we used the percentile of soil moisture to represent the relative wetness
434 of soil moisture as well as the seasonal trend of soil moisture, which was then compared
435 with the percentile of rainfall ([see supplementary and Figure S3, S4](#)). While more

436 sophisticated models can be used for soil moisture estimation, there could still be
437 substantial uncertainties (Ran et al 2020). Yet the seasonal trend and the relative
438 magnitude, after averaging through long-term records would be less impacted by the
439 simplification in estimation (Berghuijs et al 2019; Zhang et al 2019).

440 Our findings may appear different from that in Yang et al (2020), which attributed
441 the dominant flood generation mechanism in the Yangtze River basin to rainfall. This
442 may be explained by different classification criteria: Yang et al (2020) considered both
443 short-rain and long-rain as rainfall impacts while here we only considered the daily
444 rainfall. Thus, the importance of antecedent soil moisture may be considered as long-
445 rain impacts in Yang et al (2020). It is possible that soil moisture at the day before the
446 AMFs may not be the soil moisture before the event in large catchments due to the long
447 concentration time. We estimated the concentration time for 10 sites with largest
448 drainage area (larger than 100,000 km²): the ones on the main stream and at the outlets
449 of major tributaries following the USBR method (USBR 1973; Gericke & Smithers
450 2014). The concentration time is mostly within two days for main stream sites and is
451 less than 24hr for sites at the outlets of major tributaries (Table S1). Since the rest of
452 the sites are all smaller than these ones, so would be the concentration time. That is, for
453 the natural watersheds we focused on, the concentration time is likely to be within one
454 day. Thus, the soil moisture at the day before AMFs would contribute to the generation
455 of AMFs, and should be applicable for this study.

456 Besides, the exchange with groundwater was not considered in the soil moisture
457 estimation. The exchange with groundwater is more complicated and heterogenous (i.e.,
458 rivers could receive groundwater recharge in hilly area and recharge groundwater in
459 lower land (Che et al 2021)). According to Huang et al. (2021), the variation of

460 groundwater level in the Yangtze River basin is relatively small. Since the goal of this
461 study is to capture the first order seasonal variation of soil moisture and develop a
462 framework that differentiates the relative importance of precipitation and soil moisture
463 in flood generation, in this study, we estimated the soil moisture following Berhuijs (et
464 al 2016, 2019) with a simple water balance equation.

465 Moreover, this work is focused on the relative importance soil moisture and rainfall,
466 the impact of snowmelt is not considered due to the warm and humid climate in the
467 study watersheds. To apply our findings to cold watersheds with significant impact of
468 snow, the snowmelt component needs to be incorporated. In addition, our method is
469 based on the average values from many years. While previous work indicated that the
470 occurrence of floods in our study watersheds are highly concentrated (Wang et al 2021),
471 there could be strong inter-annual variability in other watersheds. In future studies,
472 annual scale and event scale analysis are needed to examine and improve our findings
473 before it can be applied to watersheds with more diverse climate and landscape
474 conditions. There could be uncertainties embedded in the estimation of soil moisture
475 due to the uncertainties in the inputs and model structures. Comprehensive evaluation
476 of the performance and uncertainty is beyond the scope of our study. More sophisticated
477 models with groundwater component, remote sensing data, and reanalysis product with
478 higher spatial-temporal resolution are needed to provide more accurate estimation and
479 further validation of soil moisture, ET, and advances our understandings of the flood-
480 generation SPR.

481 **5 Conclusions**

482 Heavy rainfall on highly saturated soil was identified as the dominant flood generation
483 mechanism across world (Berghuijs et al 2019; Wang et al 2021; Wasko et al 2020).

484 This study aims to further evaluate the relative importance of antecedent soil moisture
485 and rainfall on floods generation and the controlling factors. Climate and hydrological
486 data from 224 hydrological stations and 247 meteorological stations in the middle and
487 lower reaches of the Yangtze River basin was analyzed, along with the modeled soil
488 moisture. Except the regulated watersheds, the relative importance of antecedent soil
489 moisture and daily rainfall present significant correlation with drainage area: the larger
490 the watershed is, the more essential antecedent soil saturation rate is in flood generation,
491 the less important daily rainfall is.

492 Using the percentile of antecedent soil moisture and rainfall as coordinates, the
493 flood generation mechanism(s) of study watersheds could be grouped into three classes:
494 antecedent soil moisture dominated large flat watersheds, heavy rainfall dominated
495 steep and small to middle size watersheds, and small to middle size watersheds with
496 gentle topographic gradient where floods occurrence requires both highly saturated soil
497 and heavy rainfall. Our analysis further shows that the ratio of relative importance
498 between antecedent soil moisture and rainfall (SPR) can be predicted by topographic
499 wetness index. When the topographic wetness index is large, the dominance of
500 antecedent soil moisture for extreme floods is stronger, and *vice versa*. The SPR also
501 presents negative correlation with area normalized flood peak.

502 With the potential increase of extreme rainfall events (Gao et al., 2016; Chen et
503 al., 2016), upstream mountainous watersheds in the middle and lower Yangtze River
504 basin are facing higher risk of extreme floods. The lack of hydrological records further
505 increases the vulnerability of people in these watersheds. The flood risks could be
506 reduced by construction of flood control facilities, but it is difficult to set flood control
507 standards in these ungauged watersheds. Our findings provide a framework to

508 quantitatively estimate the possible flood risk for these ungauged watersheds. Based on
509 measurable watershed characteristics (i.e., drainage area and topographic gradient), the
510 flood generation SPR could be derived, which could then be used to estimate the mean
511 annual flood. This information can provide scientific support for flood control
512 management as well as infrastructures construction.

513 Future analysis at event scale could help generate the flood-generation curve
514 between SPR and discharge at event scale to further improve flood risk predictions in
515 these small ungauged watersheds. With more data from other regions and improved
516 estimation or observation of soil moisture, we could expand our analysis to watersheds
517 with more diverse climate and topographic characteristics to examine and refine our
518 findings and to enhance our understandings of flood generation. Comparison between
519 different time periods (i.e., before and after 2000) could also reveal temporal changes
520 in floods generation, which may be linked to the climate change, yet longer data records
521 are needed to generate representative patterns.

522

523 **Data availability**

524 DEM data was downloaded from Geospatial Data Cloud at <http://www.gscloud.cn/>.
525 Climatological data used in this study was obtained from China Meteorological Data
526 Network, which can be accessed at <http://data.cma.cn/>. Discharge data comes from
527 Annual Hydrological Report of the People's Republic of China issued by Yangtze River
528 Water Resources Commission.

529

530 **Acknowledgements**

531 This research was funded by the National Key Research and Development Program of
532 China (2019YFC1510701-01), and National Natural Science Foundation of China
533 (51979243).

534

535 **References**

- 536 Abbas, S.A., Xuan, Y. and Song, X.: Quantile Regression Based Methods for
537 Investigating Rainfall Trends Associated with Flooding and Drought Conditions.
538 Water Resources Management, 33(12), 4249-4264, [https://doi:10.1007/s11269-](https://doi:10.1007/s11269-019-02362-0)
539 019-02362-0, 2019.
- 540 Alfonso R., Nilza M. R.C., and Anderson L. R.: Numerical Modelling of the
541 Topographic Wetness Index: An Analysis at Different Scales, International
542 Journal of Geosciences(4), 476-483, [https:// doi:10.4236/ijg.2011.24050](https://doi:10.4236/ijg.2011.24050), 2011.
- 543 Allen R. G., Pereira L. S. and Races D.: Crop evapotranspiration-Guidelines for
544 computing crop water requirements FAO Irrigation and drainage paper
545 NO.56(Electric Publication)[M], Rome , Italy:FAO, 1998.
- 546 Bennett, B., Leonard, M., Deng, Y., Westra, S.: An empirical investigation into the
547 effect of antecedent precipitation on flood volume. J. Hydrol. 567, 435–445.
548 <https://doi.org/10.1016/j.jhydrol.2018.10.025>, 2018.
- 549 Berghuijs, W.R., Allen, S.T., Harrigan, S. and Kirchner, J.W.: Growing Spatial Scales
550 of Synchronous River Flooding in Europe. Geophysical Research Letters, 46(3),
551 1423-1428, <https://doi:10.1029/2018GL081883>, 2019a.
- 552 Berghuijs, W.R., Harrigan, S., Molnar, P., Slater, L.J. and Kirchner, J.W.: The Relative
553 Importance of Different Flood-Generating Mechanisms Across Europe. Water
554 Resources Research, 55(6), 4582-4593, <https://doi:10.1029/2019WR024841>,
555 2019b.
- 556 Berghuijs, W.R., Woods, R.A., Hutton, C.J. and Sivapalan, M.: Dominant flood
557 generating mechanisms across the United States. Geophysical Research Letters,
558 43(9), 4382-4390, <https://doi:10.1002/2016GL068070>, 2016.
- 559 Bertola, M., Viglione, A., Vorogushyn, S., Lun, D., Merz, B., Blöschl, G.: Do small
560 and large floods have the same drivers of change? A regional attribution analysis
561 in Europe. Hydrol. Earth Syst. Sci. 25, 1347–1364. [https://doi.org/10.5194/hess-](https://doi.org/10.5194/hess-25-1347-2021)
562 25-1347-2021, 2021.
- 563 Blöschl, G., Nester, T., Komma, J., Parajka, J. and Perdigao, R.A.P.: The June 2013
564 flood in the Upper Danube Basin, and comparisons with the 2002, 1954, and 1899
565 floods. Hydrol. Earth Syst. Sci., 17, 5197–5212, 2013.

-
- 566 Blöschl, G., Hall, J., Parajka, J., Perdigão, R. A., Merz, B., Arheimer, B., et al.:
567 Changing climate shifts timing of European floods. *Science*, 357(6351), 588 -
568 590. <https://doi.org/10.1126/science.aan2506>, 2017.
- 569 Blöschl, G., Hall, J., Viglione, A., Perdigao, R.A., Parajka, J., Merz, B., et al.: Changing
570 climate both increases and decreases European river floods, *Nature*, 573, 108 -
571 111, 2019.
- 572 Berti, A., Tardivo, G., Chiaudani, A., Rech, F. and Borin, M.: Assessing reference
573 evapotranspiration by the Hargreaves method in north-eastern Italy. *Agricultural*
574 *Water Management*, 140, 20-25, <https://doi:10.1016/j.agwat.2014.03.015>, 2014.
- 575 Brunner, M. I., Seibert, J. and Favre, A.C.: Bivariate return periods and their importance
576 for flood peak and volume estimation. *Water*, 3, 819 - 833.
577 <https://doi.org/10.1002/wat2.1173>, 2016.
- 578 Brunner, M. I., Gilleland, E., Wood, A., Swain, D. L., and Clark, M.: Spatial
579 dependence of floods shaped by spatiotemporal variations in meteorological and
580 land - surface processes. *Geophysical Research Letters*, 47, e2020GL088000.
581 <https://doi.org/10.1029/2020GL088000>, 2020.
- 582 Brunner, M. I., Swain, D. L., Wood, R.R. et al. An extremeness threshold determines
583 the regional response of floods to changes in rainfall extremes. *Commun Earth*
584 *Environ* 2, 173. <https://doi.org/10.1038/s43247-021-00248-x>, 2021.
- 585 Cai, Q. H.: Great protection of Yangtze River and watershed ecology, *Yangtze River*
586 (01), 70-74, <https://doi:10.16232/j.cnki.1001-4179.2020.01.011>, 2020.
- 587 Cen, S.-x., Gong, Y.-f., Lai, X. and Peng, L.: The Relationship between the
588 Atmospheric Heating Source/Sink Anomalies of Asian Monsoon and
589 Flood/Drought in the Yangtze River Basin in the Meiyu Period. *Journal of*
590 *Tropical Meteorology*, 21(4), 352-360, 2015.
- 591 Che, Q., Su, X., Zheng, S., Li, Y.: Interaction between surface water and groundwater
592 in the Alluvial Plain (anqing section) of the lower Yangtze River Basin:
593 environmental isotope evidence. *Journal of Radioanalytical and Nuclear*
594 *Chemistry*, 329, 1331-1343, 2021.
- 595 Chen, Y. and Zhai, P.: Mechanisms for concurrent low-latitude circulation anomalies
596 responsible for persistent extreme precipitation in the Yangtze River Valley.

-
- 597 Climate Dynamics, 47(3-4), 989-1006, <https://doi.org/10.1007/s00382-015-2885-6>,
598 2016.
- 599 CRED (2015). The human cost of natural disasters: A global perspective: Centre for
600 research on the epidemiology of disasters.
- 601 Deb, P., Kiem, A.S. and Willgoose, G.: Mechanisms influencing non-stationarity in
602 rainfall-runoff relationships in southeast Australia. *Journal of Hydrology*, 571,
603 749-764, <https://doi.org/10.1016/j.jhydrol.2019.02.025>, 2019.
- 604 Desai, B., Maskrey, A., Peduzzi, P., De Bono, A., & Herold, C. Making Development
605 Sustainable: The Future of Disaster Risk Management. Global Assessment Report
606 on Disaster Risk Reduction <http://archive-ouverte.unige.ch/unige:78299> (UNISDR,
607 2015).
- 608 Do, H. X., Mei, Y., & Gronewold, A. D.: To what extent are changes in flood magnitude
609 related to changes in precipitation extremes? *Geophysical Research Letters*, 47,
610 e2020GL088684. <https://doi.org/10.1029/2020GL088684>, 2020.
- 611 Fang, X. and Pomeroy, J.W.: Impact of antecedent conditions on simulations of a flood
612 in a mountain headwater basin. *Hydrological Processes*, 30(16), 2754-2772,
613 <https://doi.org/10.1002/hyp.10910>, 2016.
- 614 Feng, B. F., Dai M. L. and Zhang T.: Effect of Reservoir Group Joint Operation on
615 Flood Control in the Middle and Lower Reaches of Yangtze River, *Journal of*
616 *Water Resources Research* (3), 278-284, <https://doi.org/10.12677/JWRR.2017.63033>,
617 2017.
- 618 Fu, G., Yu, J., Yu, X., Ouyang, R., Zhang, Y., Wang, P., Liu, W. and Min, L.: Temporal
619 variation of extreme rainfall events in China, 1961-2009. *Journal of Hydrology*,
620 487, 48-59, <https://doi.org/10.1016/j.jhydrol.2013.02.021>, 2013.
- 621 Gao, T. and Xie, L.: Spatiotemporal changes in precipitation extremes over Yangtze
622 River basin, China, considering the rainfall shift in the late 1970s. *Global and*
623 *Planetary Change*, 147, 106-124, <https://doi.org/10.1016/j.gloplacha.2016.10.016>,
624 2016.
- 625 Gao, Y., Wang, H., Lu, X., Xu, Y., Zhang, Z. and Schmidt, A.R.: Hydrologic Impact
626 of Urbanization on Catchment and River System Downstream from Taihu Lake.
627 *Journal of Coastal Research*, 82-88, <https://doi.org/10.2112/SI84-012.1>, 2018.

628 Garg, S., & Mishra, V.: Role of extreme precipitation and initial hydrologic conditions
629 on floods in Godavari river basin, India. *Water Resources Research*, 55, 9191 –
630 9210. <https://doi.org/10.1029/2019WR025863>, 2019.

631 Grabs, T., Seibert, J., Bishop, K. and Laudon, H.: Modeling spatial patterns of saturated
632 areas: A comparison of the topographic wetness index and a dynamic distributed
633 model. *Journal of Hydrology*, 373(1-2), 15-23,
634 <https://doi.org/10.1016/j.jhydrol.2009.03.031>, 2009.

635 Huang, C., Zhou, Y., Zhang, S., Wang, J., Liu, F., Gong, C., Yi, C., Li, L., Zhou, H.,
636 Wei, L., Pan, X., Shao, C., Li, Y., Han, W., Yin, Z., and Li, X.: Groundwater
637 resources in the Yangtze River Basin and its current development and utilization[J].
638 *Geology of China*, 2021, 48(4):979-1000.

639 IPCC. *Managing the Risks of Extreme Events and Disasters to Advance Climate*
640 *Change Adaptation* (eds Field, C. B. et al.) (Cambridge Univ. Press, 2012).

641 Kato, K.: On the Abrupt Change in the Structure of the Baiu Front over the China
642 Continent in Late May of 1979. *Journal of the Meteorological Society of Japan*,
643 63(1), 20-36, https://doi.org/10.2151/jmsj1965.63.1_20, 1985.

644 Kazuki, T., Oliver C. S. V., Masahiro, R.: Spatial variability of precipitation and soil
645 moisture on the 2011 flood at chao phraya river basin. *International Water*
646 *Technology Association, Proceedings of Hydrology and Water Resources*, B, 17-
647 21, 2013.

648 Kemter, M., Merz, B., Marwan, N., Vorogushyn, S., & Blöschl, G.: Joint trends in flood
649 magnitudes and spatial extents across Europe. *Geophysical Research Letters*, 47,
650 e2020GL087464. <https://doi.org/10.1029/2020GL087464>, 2020.

651 Lehner, B., C. Reidy Liermann, C. Revenga, C. Vörösmarty, B. Fekete, P. Crouzet, P.
652 Döll, M. Endejan, K. Frenken, J. Magome, C. Nilsson, J.C. Robertson, R. Rodel,
653 N. Sindorf, and D. Wisser. 2011. High-resolution mapping of the world's
654 reservoirs and dams for sustainable river-flow management. *Frontiers in Ecology*
655 *and the Environment* 9 (9): 494-502.

656 Li, Q., Wei, F. and Li, D.: Interdecadal variation of East Asian summer monsoon and
657 drought/flood distribution over eastern China in the last 159 years. *Journal of*
658 *Geographical Sciences*, 21(4), 579-593, <https://doi.org/10.1007/s11442-011-0865-2>,
659 2011.

-
- 660 Li, X., Zhang, K., Gu, P., Feng, H., Yin, Y., Chen, W. and Cheng, B.: Changes in
661 precipitation extremes in the Yangtze River Basin during 1960-2019 and the
662 association with global warming, ENSO, and local effects. *Science of the Total*
663 *Environment*, 760, <https://doi:10.1016/j.scitotenv.2020.144244>, 2021.
- 664 Liu, B., Yan, Y., Zhu, C., Ma, S., & Li, J.: Record - breaking Meiyu rainfall around the
665 Yangtze River in 2020 regulated by the subseasonal phase transition of the North
666 Atlantic Oscillation. *Geophysical Research Letters*, 47, e2020GL090342.
667 <https://doi.Org/10.1029/2020GL090342>, 2020.
- 668 Liu, L., Ye, S., Chen, C., Pan, H. and Ran, Q.: Nonsequential Response in Mountainous
669 Areas of Southwest China. *Frontiers in Earth Science*, 9: 1-15. doi:
670 10.3389/feart.2021.660244, 2021
- 671 Liu, N., Jin, Y. and Dai, J.: Variation of Temperature and Precipitation in Urban
672 Agglomeration and Prevention Suggestion of Waterlogging in Middle and Lower
673 Reaches of Yangtze River. 3rd International Conference on Energy Equipment
674 Science and Engineering (Iceese 2017), 128, [https://doi:10.1088/1755-](https://doi:10.1088/1755-1315/128/1/012165)
675 [1315/128/1/012165](https://doi:10.1088/1755-1315/128/1/012165), 2018.
- 676 Liu, S., Huang, S., Xie, Y., Wang, H., Leng, G., Huang, Q., Wei, X., and Wang, L.:
677 Identification of the Non-stationarity of Floods: Changing Patterns, Causes, and
678 Implications, *Water Resour. Manag.*, 33, 939–953, 2018.
- 679 Liu, Y., Xinyu, L., Liancheng, Z., Yang, L., Chunrong, J., Ni, W. and Juan, Z.:
680 Quantifying rain, snow and glacier meltwater in river discharge during flood
681 events in the Manas River Basin, China. *Natural Hazards*, 108(1), 1137-1158,
682 <https://doi:10.1007/s11069-021-04723-8>, 2021.
- 683 Long, L.H., Ji, D.B., Yang, Z.Y., Cheng, H.Q., Yang, Z.J., Liu, D.F., Liu, L. and Lorke,
684 A.: Tributary oscillations generated by diurnal discharge regulation in Three
685 Gorges Reservoir. *Environmental Research Letters*, 15(8),
686 <https://doi:10.1088/1748-9326/ab8d80>, 2020.
- 687 Lu, M., Wu, S.-J., Chen, J., Chen, C., Wen, Z. and Huang, Y.: Changes in extreme
688 precipitation in the Yangtze River basin and its association with global mean
689 temperature and ENSO. *International Journal of Climatology*, 38(4), 1989-2005,
690 <https://doi:10.1002/joc.5311>, 2018.

691 Meles, M.B., Younger, S.E., Jackson, C.R., Du, E., Drover, D.: Wetness index based
692 on landscape position and topography (WILT): Modifying TWI to reflect
693 landscape position, *Journal of Environmental Management* 255, 109863, 2020.

694 Miao, Q., Huang, M. and Li, R., Q.: Response of net primary productivity of vegetation
695 in Yangtze River Basin to future climate change. *Journal of Natural Resources*, 25,
696 08(2010):1296-1305, doi:CNKI:SUN:ZRZX.0.2010-08-007, 2015.

697 Munoz, S.E., Giosan, L., Therrell, M.D., Remo, J.W.F., Shen, Z., Sullivan, R.M.,
698 Wiman, C., O'Donnell, M., and Donnelly, J.P.: Climatic control of Mississippi
699 River flood hazard amplified by river engineering, 556, 95 – 98, 2018.

700 Musselman, K.N., Lehner, F., Ikeda, K., Clark, M.P., Prein, A.F., Liu, C., Barlage, M.
701 and Rasmussen, R.: Projected increases and shifts in rain-on-snow flood risk over
702 western North America, *Nature Climate Change*, 8, 808 – 812, 2018.

703 Ockert J. G. and Jeff C. S.: Review of methods used to estimate catchment response
704 time for the purpose of peak discharge estimation, *Hydrological Sciences Journal*,
705 59:11, 1935-1971, DOI: 10.1080/02626667.2013.866712, 2014.

706 Ohmura, A. and Wild, M.: Is the hydrological cycle accelerating? *Science*, 298, 1345 –
707 1346, 2002.

708 Pegram, G. and Bardossy, A.: Downscaling Regional Circulation Model rainfall to
709 gauge sites using recorrelation and circulation pattern dependent quantile-quantile
710 transforms for quantifying climate change. *Journal of Hydrology*, 504, 142-159,
711 <https://doi:10.1016/j.jhydrol.2013.09.014>, 2013.

712 Peng, T., Tian, H., Singh, V. P., Chen, M., Liu, J., Ma, H. B. and Wang, J. B.:
713 Quantitative assessment of drivers of sediment load reduction in the Yangtze River
714 basin, China, *Journal of Hydrology*, 580,
715 <https://doi:10.1016/j.jhydrol.2019.124242>, 2020.

716 Qian, H. and Xu, S.-B.: Prediction of Autumn Precipitation over the Middle and Lower
717 Reaches of the Yangtze River Basin Based on Climate Indices. *Climate*, 8(4),
718 <https://doi:10.3390/cli8040053>, 2020.

719 Ran, Q., Chen, X., Hong Y., Ye S., and Gao J.: Impacts of terracing on hydrological
720 processes: A case study from the Loess Plateau of China. *Journal of Hydrology*,
721 588, <https://doi:10.1016/j.jhydrol.2020.125045>, 2020.

722 Ran, Q., Zong, X., Ye, S., Gao, J. and Hong, Y.: Dominant mechanism for annual
723 maximum flood and sediment events generation in the Yellow River basin. *Catena*,
724 187, <https://doi:10.1016/j.catena.2019.104376>, 2020.

725 Ray S. M., Ramakar J. and Kishanjit K. K.: Precipitation-runoff simulation for a
726 Himalayan River Basin, India using artificial neural network algorithms, *Sciences*
727 *in Cold and Arid Regions*, 5(1), 85-95, 2013.

728 Rottler, E., Francke, T., Burger, G., and Bronstert, A.: Long-term changes in central
729 European river discharge for 1869 – 2016: impact of changing snow covers,
730 reservoir constructions and an intensified hydrological cycle, *Hydrol. Earth Syst.*
731 *Sci.*, 24, 1721 – 1740, 2020.

732 Smith, J. A., Cox, A. A., Baeck, M. L., Yang, L., and Bates, P.: Strange floods: the
733 upper tail of flood peaks in the United States, *Water Resour. Res.*, 54, 6510 – 6542,
734 2018.

735 Sorensen, R., Zinko, U., and Seibert, J.: On the calculation of the topographic wetness
736 index: evaluation of different methods based on field observations, *Hydrology and*
737 *Earth System Sciences*, 10, 101–112, 2006.

738 Su, Z., Ho, M., Hao, Z., Lall, U., Sun, X., Chen, X. and Yan, L.: The impact of the
739 Three Gorges Dam on summer streamflow in the Yangtze River Basin.
740 *Hydrological Processes*, 34(3), 705-717, <https://doi:10.1002/hyp.13619>, 2020.

741 Suresh, S. S., Benefit O., Augustine T., and Trevor P.: Peoples’ Perception on the
742 Effects of Floods in the Riverine Areas of Ogbia Local Government Area of
743 Bayelsa State, Nigeria, *Knowledge Management*, [https://doi:10.18848/2327-](https://doi:10.18848/2327-7998/CGP/v12i02/50793)
744 [7998/CGP/v12i02/50793](https://doi:10.18848/2327-7998/CGP/v12i02/50793), 2013.

745 Tao, S. Y., *Rainstorm in China* [M], Beijing: Science Press, 1980.(in Chinese)

746 Trambly, Y., Villarini, G., El Khalki, E. M., Gründemann, G., & Hughes, D.:
747 Evaluation of the drivers responsible for flooding in Africa. *Water Resources*
748 *Research*, 57, e2021WR029595. <https://doi.Org/10.1029/2021WR029595>, 2021.

749 USBR (United States Bureau of Reclamation), 1973. *Design of small dams*. 2nd ed.
750 Washington, DC: Water Resources Technical Publications.

751 Vicente-Serrano, S.M., Azorin-Molina, C., Sanchez-Lorenzo, A., Revuelto, J., Lopez-
752 Moreno, J.I., Gonzalez-Hidalgo, J.C., Moran-Tejeda, E. and Espejo, F.: Reference
753 evapotranspiration variability and trends in Spain, 1961-2011. *Global and*
754 *Planetary Change*, 121, 26-40, <https://doi:10.1016/j.gloplacha.2014.06.005>, 2014.

-
- 755 Volpi, E., Di Lazzaro, M., Bertola, M., Viglione, A. and Fiori, A.: Reservoir Effects on
756 Flood Peak Discharge at the Catchment Scale. *Water Resources Research*, 54(11),
757 9623-9636, <https://doi:10.1029/2018wr023866>, 2018.
- 758 Wang, H., Zhou, Y., Pang, Y. and Wang, X.: Fluctuation of Cadmium Load on a Tide-
759 Influenced Waterfront Lake in the Middle-Lower Reaches of the Yangtze River.
760 *Clean-Soil Air Water*, 42(10), 1402-1408, <https://doi:10.1002/clen.201300693>,
761 2014.
- 762 Wang, J., Ran, Q., Liu, L., Pan, H. and Ye, S.: Study on the Dominant Mechanism of
763 Extreme Flow Events in the Middle and Lower Reaches of the Yangtze River,
764 *China Rural Water and Hydropower*, Accepted.
- 765 Wang, R., Yao, Z., Liu, Z., Wu, S., Jiang, L. and Wang, L.: Snow cover variability and
766 snowmelt in a high-altitude ungauged catchment. *Hydrological Processes*, 29(17),
767 3665-3676, <https://doi:10.1002/hyp.10472>, 2015.
- 768 Wang, W., Xing W., Yang, T., Shao, Q., Peng, S., Yu, Z., and Yong, B.: Characterizing
769 the changing behaviours of precipitation concentration in the Yangtze River Basin,
770 China. *Hydrological Processes*, 27(24), 3375-3393, <https://doi:10.1002/hyp.9430>,
771 2013.
- 772 Wang, Z. and Plate, E.: Recent flood disasters in China. *Proceedings of the Institution*
773 *of Civil Engineers – Water and Maritime Engineering* (3),
774 <https://doi:10.1680/wame.2002.154.3.177>, 2002.
- 775 Wasko, C. and Nathan, R.: Influence of changes in rainfall and soil moisture on trends
776 in flooding. *Journal of Hydrology*, 575, 432-441,
777 <https://doi:10.1016/j.jhydrol.2019.05.054>, 2019.
- 778 Wasko, C., Nathan, R., & Peel, M. C.: Changes in antecedent soil moisture modulate
779 flood seasonality in a changing climate. *Water Resources Research*, 56,
780 e2019WR026300. <https://doi.org/10.1029/2019WR026300>, 2020.
- 781 Wasko, C., Nathan, R., Stein, L., O'Shea, D.: Evidence of shorter more extreme
782 rainfalls and increased flood variability under climate change. *J. Hydrol.* 603,
783 126994. <https://doi.org/10.1016/j.jhydrol.2021.126994>, 2021.
- 784 Wu, X. S., Guo, S. L. and Ba, H. H.: Long-term precipitation forecast method based on
785 SST multipole index, *Journal of water conservancy*(10), 1276-1283,
786 <https://doi:10.13243/j.cnki.slxb.20180544>, 2018.

787 Xia, J. and Chen, J.: A new era of flood control strategies from the perspective of
788 managing the 2020 Yangtze River flood. *Science China-Earth Sciences*, 64(1), 1-
789 9, <https://doi:10.1007/s11430-020-9699-8>, 2021.

790 Xie, Z., Du, Y., Zeng, Y. and Miao, Q.: Classification of yearly extreme precipitation
791 events and associated flood risk in the Yangtze-Huaihe River Valley. *Science*
792 *China-Earth Sciences*, 61(9), 1341-1356, <https://doi:10.1007/s11430-017-9212-8>,
793 2018.

794 Yang, H.F., Yang, S.L., Xu, K.H., Milliman, J.D., Wang, H., Yang, Z., Chen, Z. and
795 Zhang, C.Y.: Human impacts on sediment in the Yangtze River: A review and new
796 perspectives. *Global and Planetary Change*, 162, 8-17,
797 <https://doi:10.1016/j.gloplacha.2018.01.001>, 2018.

798 Yang, L., Wang, L., Li, X. and Gao, J.: On the flood peak distributions over China.
799 *Hydrology and Earth System Sciences*, 23(12), 5133-5149,
800 <https://doi:10.5194/hess-23-5133-2019>, 2019.

801 Yang, W., Yang, H., and Yang, D.: Classifying floods by quantifying driver
802 contributions in the Eastern Monsoon Region of China, *Journal of Hydrology*, 585,
803 124767, 2020.

804 Yang, W., Yang, H., Yang, D., and Hou, A.: Causal effects of dams and land cover
805 changes on flood changes in mainland China. *Hydrol. Earth Syst. Sci.*, 25, 2705–
806 2720, 2021.

807 Ye, S., Li, H., Leung, L.R., Guo, J., Ran, Q., Demissie, Y., et al., 2017. Understanding
808 flood seasonality and its temporal shifts within the contiguous United States. *J.*
809 *Hydrometeorol.* 18 (7), 1997 – 2009.

810 Ye, X., Xu, C.-Y., Li, Y., Li, X. and Zhang, Q.: Change of annual extreme water levels
811 and correlation with river discharges in the middle-lower Yangtze River:
812 Characteristics and possible affecting factors. *Chinese Geographical*
813 *Science*, 27(2), 325-336, <https://doi:10.1007/s11769-017-0866-x>, 2017.

814 Yu, F., Chen, Z., Ren, X. and Yang, G.: Analysis of historical floods on the Yangtze
815 River, China: Characteristics and explanations. *Geomorphology*, 113(3-4), 210-
816 216, <https://doi:10.1016/j.geomorph.2009.03.008>, 2009.

817 Zhang, H., Liu, S., Ye, J. and Yeh, P.J.F.: Model simulations of potential contribution
818 of the proposed Huangpu Gate to flood control in the Lake Taihu basin of China.

819 Hydrology and Earth System Sciences, 21(10), 5339-5355,
820 <https://doi:10.5194/hess-21-5339-2017>, 2017.

821 Zhao, J., Li, J., Yan, H., Zheng, L. and Dai, Z.: Analysis on the Water Exchange
822 between the Main Stream of the Yangtze River and the Poyang Lake. 2011 3rd
823 International Conference on Environmental Science and Information Application
824 Technology Esiat 2011, Vol 10, Pt C,10, 2256-2264,
825 <https://doi:10.1016/j.proenv.2011.09.353>, 2011.

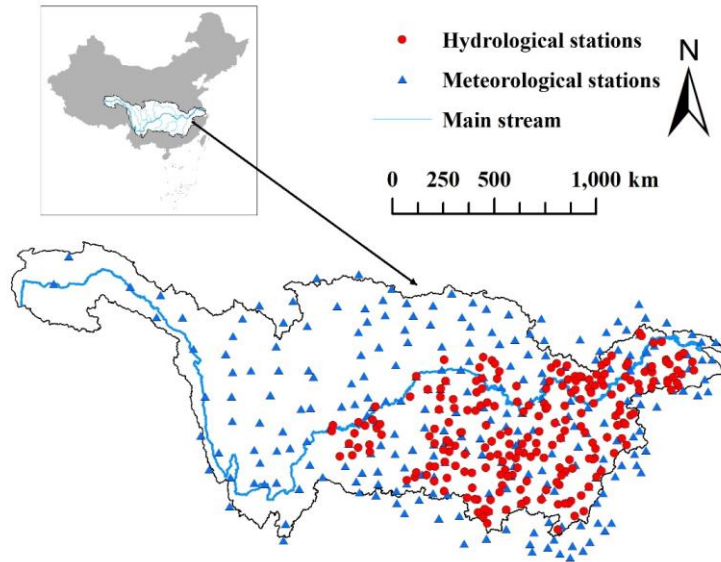
826 Zhang, S., Kang, L. and He, X.: Equal proportion flood retention strategy for the leading
827 multireservoir system in upper Yangtze River. International Conference on Water
828 Resources and Environment, WRE 2015, 2015.

829 Zhang, W., Villarini, G., Vecchi, G.A. and Smith, J. A.: Urbanization exacerbated the
830 rainfall and flooding caused by hurricane Harvey in Houston. *Nature*, 563, 384 –
831 388, 2018.

832 Zhang, K., Wang, Q., Chao, L., Ye, J., Li, Z., Yu, Z., Yang, T. and Ju, Q.: Ground
833 observation-based analysis of soil moisture spatiotemporal variability across a
834 humid to semi-humid transitional zone in China. *Journal of Hydrology*, 574, 903-
835 914, 2019.

836 Zou, B., Li, Y., Feng, B.: Analysis on dispatching influence of Three Gorges Reservoir
837 on water level of main stream in mid-lower reaches of Yangtze River: a case study
838 of flood in July,2010. *Yangtze River*, 42.06:80-82+100. doi:10.16232/j.cnki.1001-
839 4179.2011.06.004, 2011.

840
841



842

843 **Figure 1:** Map of the Yangtze River basin, and the meteorological stations and
844 hydrological stations. The blue line is the main stream of Yangtze River.

845

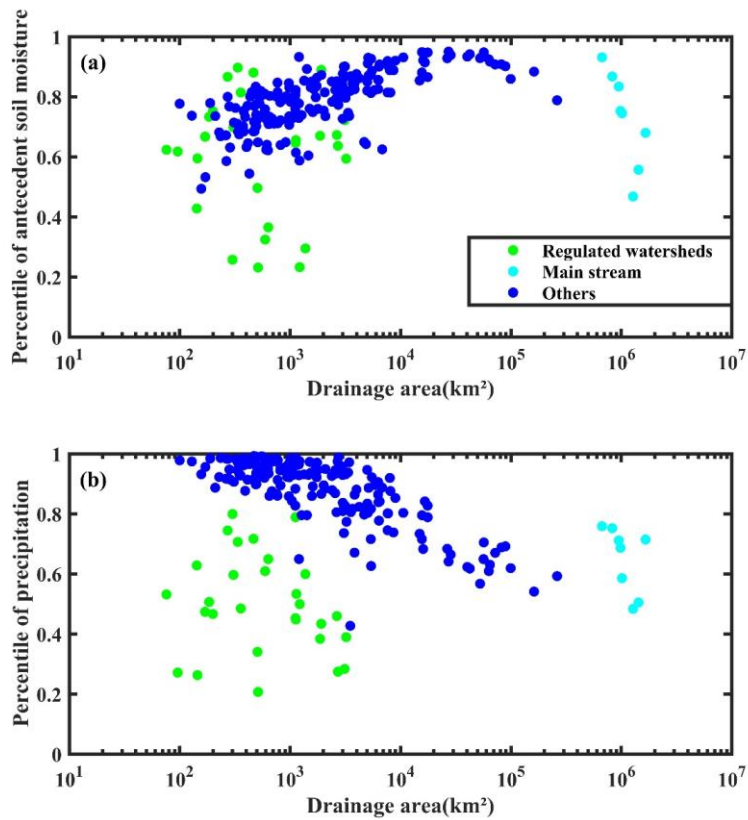


(a) Percentile of antecedent soil moisture

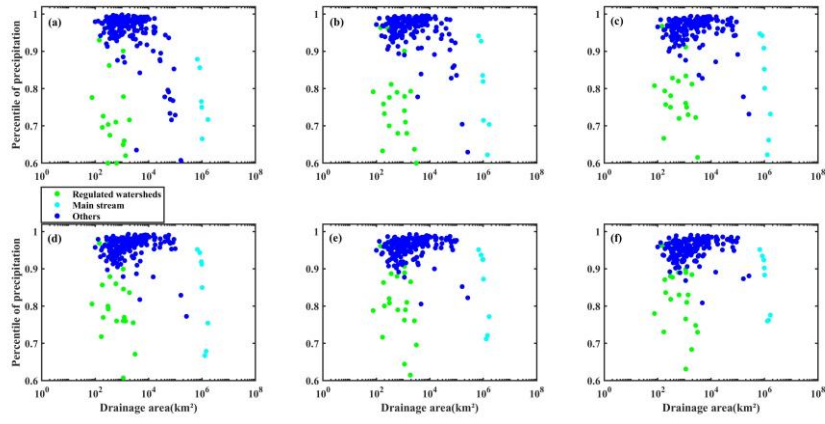


(b) Percentile of precipitation

846
847 **Figure 2:** The spatial distribution of (a) the percentile of antecedent soil moisture during
848 annual maximum flood; (b) the percentile of daily precipitation during annual
849 maximum flood.
850



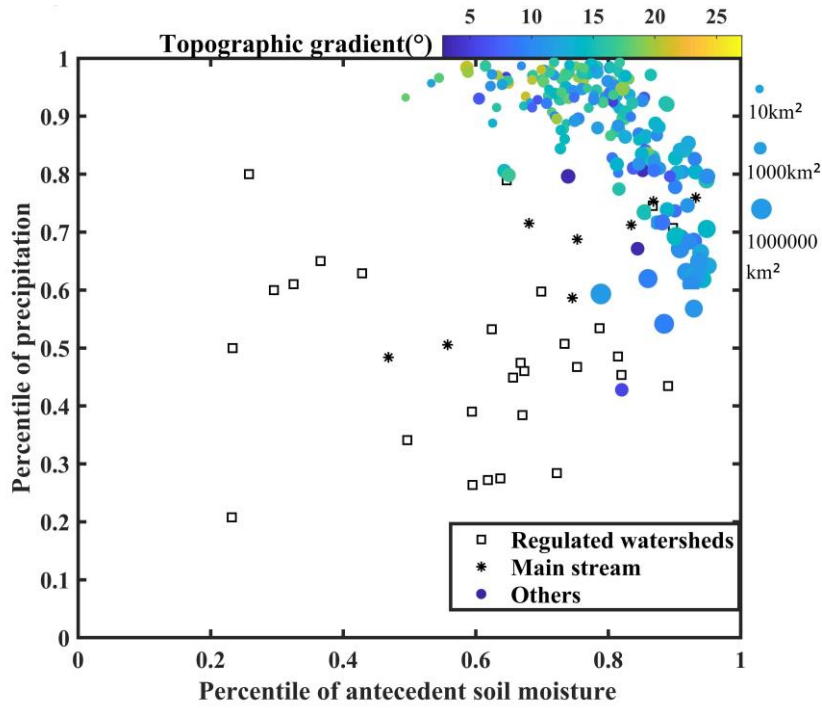
851
 852 **Figure 3:** Scatterplot between the drainage area and (a) the percentile of antecedent soil
 853 moisture of AMF events (the linear regression for blue dots: $R^2 = 0.46$, p -value<0.001);
 854 (b) the percentile of precipitation at the day of AMF events (the linear regression for
 855 blue dots: $R^2 = 0.61$, p -value<0.001). The green dots represent the regulated watershed,
 856 the cyan dots represent the sites on the main stream, and the rest sites are shown in blue.
 857
 858
 859



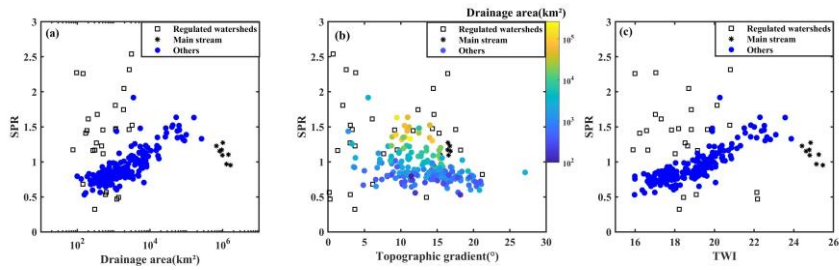
860

861 **Figure 4:** Scatterplot between the drainage area and the percentile of accumulated
 862 rainfall of (a) two days; (b) three days; (c) four days; (d) five days; (e) six days; and (f)
 863 seven days on AMF events.

864



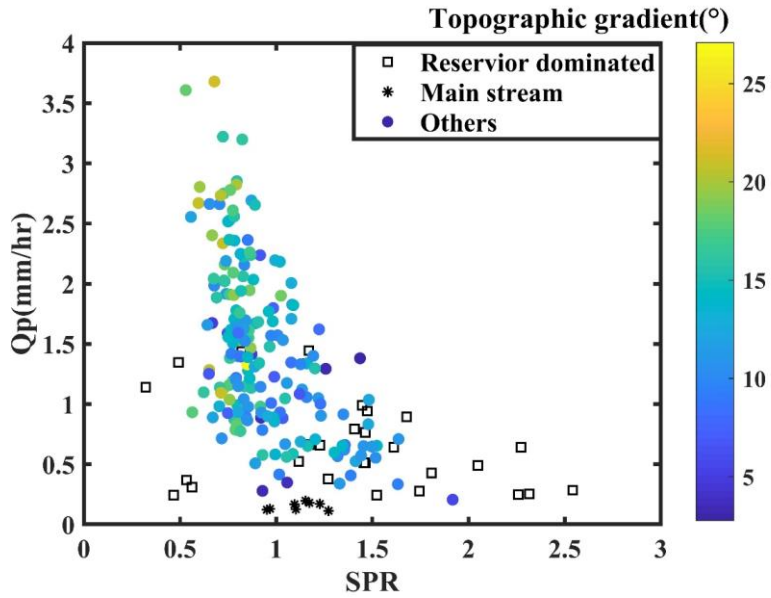
865
 866 **Figure 5:** Scatterplot of the percentile of precipitation and antecedent soil moisture, the
 867 color represents topographic gradient and the size of circles is scaled by drainage area.
 868
 869



870

871 **Figure 6:** Scatterplots between the ratio of antecedent soil moisture and precipitation
 872 (SPR) and (a) drainage area; (b) topographic gradient; and (c) topographic wetness
 873 index (TWI).

874



875

876 **Figure 7:** Scatterplot between the ratio of antecedent soil moisture and precipitation
877 (SPR) and area weighted annual maximum discharge (Q_p), the color represents
878 topographic gradient.

879

Supplementary

To validate our results, we collected the 0-200cm soil moisture from the China Land Data Assimilation System (CLDAS) provided by China Meteorological Administration (CMA) (Wang & Li 2020). 37 catchments covering a range of climate and topography were selected for comparison (Figure S3). Since this dataset only has soil moisture data from 2008, the mean percentile of antecedent soil moisture was calculated from 2008 to 2016 based on the CLDAS soil moisture. This was then compared with the mean percentile based on water balance as in the manuscript (Figure S4). As we can see from Figure S4, the scatters fall around the 1:1 line, that is, the mean percentile calculated from water balance are close to the mean percentile from re-analysis soil moisture. This is consistent with our discussion that averaging through long-term records would be less impacted by the simplification in estimation. Due to the length of CLDAS dataset, we only averaged within 9 years, for the at least 25 years records used in our study, it is likely to be less scatter. While this is just a minimal evaluation of the values, given the goal of this study, we think the averaged percentile of antecedent soil moisture based on the water balance model is acceptable for the purpose of this study at the mean annual scale.

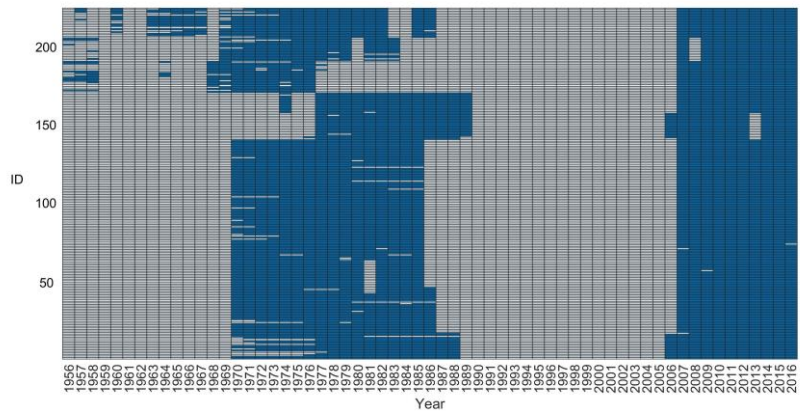
Wang, Y. and Li, G. (2020). Evaluation of simulated soil moisture from China Land Data Assimilation System (CLDAS) land surface models, Remote Sensing Letters, 11 (12), 1060 – 1069.

带格式的: 左侧: 3.17 厘米, 右侧: 3.17 厘米, 指定行和字符网格

25 **Table S1:** Estimated concentration time for 10 sites with largest drainage area: the ones
26 on main stream (MS) and the ones at the outlets of major tributaries (TR).
27

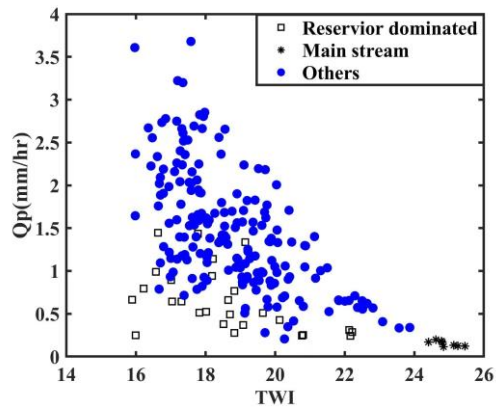
Site Name	Concentration Time (hr)	Drainage Area (km ²)
TR-Hukou	17.9	161,979
TR-Chenglingji	18.8	261,986
MS-Zhutuo	32.7	668,661
MS-Cuntan	32.8	827,799
MS-Wanxian	37.6	948,524
MS-Yichang	41.5	982,948
MS-Jianli	45.2	1,014,690
MS-Luoshan	46.3	1,276,676
MS-Hankou	51.0	1,432,008
MS-Datong	54.3	1,657,604

28
29
30
31



32
33
34
35

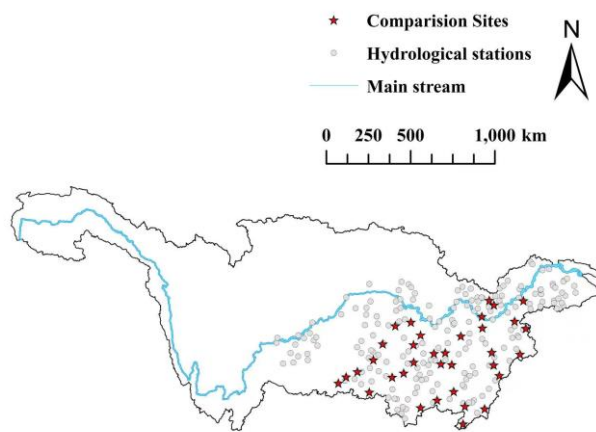
Figure S1: The data availability of each station, each column indicates each year while each row is corresponding to each station, blue grid indicates there is record of this year.



36

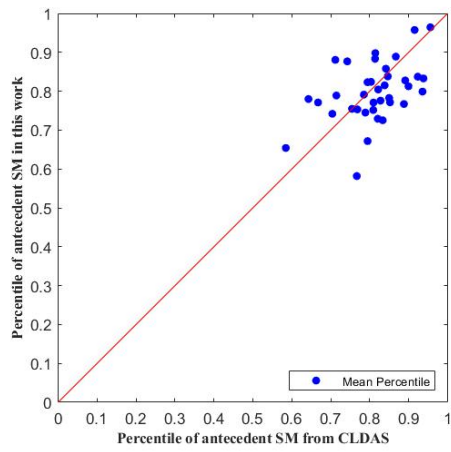
37 **Figure S2:** Scatterplot between the topographic wetness index (TWI) and area weighted
38 annual maximum discharge (Q_p).

39



40
41
42

Figure S3: Map of the 37 selected stations used for comparison.



43
44
45
46
47
48
49

Figure S4: Comparison between the mean percentile of antecedent soil moisture in our work and the percentile of antecedent soil moisture from re-analysis dataset CLDAS (China Land Data Assimilation System). The red line is the 1:1 line.